

# Non-cyanobacterial diazotrophs dominate dinitrogen fixation in biological soil crusts at the early stage of crust formation.

Charles Pepe-Ranney<sup>1</sup>, Chantal Koechli<sup>1</sup>, Ruth Potrafka<sup>2</sup>, Ferran Garcia-Pichel<sup>2</sup>, Daniel H Buckley<sup>1,\*</sup>

<sup>1</sup>Cornell University, Department of Crop and Soil Sciences, Ithaca, NY, USA

<sup>2</sup>Arizona State University, School of Life Sciences, Tempe, AZ 85287, USA.

Correspondence\*:

Daniel H Buckley

Cornell University, Department of Crop and Soil Sciences, Ithaca, NY, USA,

## 1 ABSTRACT

Biological soil crusts (BSC) cover a vast global area and are key components of ecosystem productivity in arid soils. In particular, BSC contribute significantly to the nitrogen (N) budget in arid ecosystems via N<sub>2</sub>-fixation. N<sub>2</sub>-fixation in mature crusts is largely attributed to heterocystous cyanobacteria, however, early successional crusts possess few N-fixing cyanobacteria and this suggests that microorganisms other than cyanobacteria mediate N<sub>2</sub>-fixation during the early stages of BSC development. DNA stable isotope probing (DNA-SIP) with <sup>15</sup>N<sub>2</sub> revealed that *Clostridiaceae* and *Proteobacteria* are the most common microorganisms to assimilate <sup>15</sup>N in early successional 'light' crusts. The maximum relative abundance of non-cyanobacterial <sup>15</sup>N<sub>2</sub>-assimilating taxa in environmental BSC SSU rRNA gene sequence collections was 0.00225% and 0.00127% for taxa that belong to *Clostridiaceae* and *Proteobacteria*, respectively. Their low abundance may explain why these heterotrophic diazotrophs have not previously been characterized in BSC. Diazotrophs play a critical role in BSC formation and characterization of these organisms represents a crucial step towards understanding how anthropogenic change will effect the formation and ecological function of BSC in arid ecosystems.

## 2 INTRODUCTION

Biological soil crusts (BSC) are specialized microbial mat communities that form at the soil surface in arid environments and fill a variety of important ecological functions in arid ecosystems. BSC occupy plant interspaces and cover a wide, global geographic range (Garcia-Pichel et al., 2003b). The ground cover of BSC on the Colorado Plateau has been measured as high as 80% by remote sensing (Karnieli et al., 2003). The global biomass of BSC *Cyanobacteria* alone is estimated at 54 x 10<sup>12</sup> g C (Garcia-Pichel et al., 2003b). BSC play important roles in arid ecosystem productivity and are responsible for significant nitrogen (N) flux (for review of BSC N<sub>2</sub>-fixation see Belnap (2003)). N<sub>2</sub>-fixation represents the dominant source of new ecosystem N in more than 80% of BSC from diverse sites across North America, Africa, and Australia (Evans and Belnap, 1999), while atmospheric N deposition was a dominant source of N in only a minority of sites. The presence of BSC is positively correlated with vascular plant survival due in part to BSC ecosystem N contributions (for review of BSC-vascular plant interactions see Belnap et al. (2003)). Climate change and disturbance could alter BSC microbial community structure/membership and therefore it is possible that there will also be changes in diazotroph diversity and N<sub>2</sub>-fixation and that these changes can alter the BSC N-budget.

BSC N<sub>2</sub>-fixation rate studies (typically employing the acetylene reduction assay (ARA)) have explored BSC diazotroph activity across various ecological gradients. Reported BSC N<sub>2</sub>-fixation rates vary significantly across samples and studies (Evans and Lange, 2001). The reasons for inter-site and inter-study variability are complex and likely include the spatial heterogeneity of BSC (Evans and Lange, 2001) and the impact of recent environmental change on N<sub>2</sub>-fixation rates (see Belnap (2001) for discussion). Moreover, the ARA assay is subject to methodological artifacts that can complicate making robust comparisons across sample types that differ in physical and biological characteristics (see Belnap (2001) for review). Nonetheless, N<sub>2</sub>-fixation rates are consistently higher in mature BSC than in young, early successional BSC (Belnap, 2002; Yeager et al., 2004). This difference may be due to the proliferation of heterocystous *Cyanobacteria* in older mats and is consistent with the theory that heterocystous *Cyanobacteria* provide the main source of fixed-N in BSC. Alternatively, the N<sub>2</sub>-fixation rate differences between young and old BSC might be attributable to methodological artifacts. For instance, Johnson et al. (2005) show that N<sub>2</sub>-fixation in mature mats is maximal at the crust surface (coincident with heterocystous cyanobacteria) while it is maximal below the crust surface in early successional BSC. Diffusional limitation can potentially cause ARA to underestimate N<sub>2</sub>-fixation which occurs below the crust surface and as a result ARA may systematically underestimate rates of N<sub>2</sub>-fixation in early successional BSC. Diffusion would not be an issue when measuring N<sub>2</sub>-fixation rates in mature crust as nitrogenase activity peaks near the surface. Differences of N<sub>2</sub> fixation rates between developing and mature BSC were not statistically significant when aerial rates were estimated by integrating across ARA performed on thin (1-3mm) slices across a BSC depth profile Johnson et al. (2005).

Molecular studies of BSC microbial diversity include explorations of the BSC microbial community vertical profile (Garcia-Pichel et al., 2003a), BSC *nifH* gene content surveys (e.g. Yeager et al. (2004), Yeager et al. (2012), Yeager et al. (2006) and Steppe et al. (1996)), and next-generation-sequencing (NGS) enabled studies of BSC SSU rRNA gene content across wide geographic ranges (Garcia-Pichel et al., 2013; Steven et al., 2013). Early successional BSC are often described as "light" in appearance relative to "dark" mature BSC (Belnap, 2002; Yeager et al., 2004). Mature BSC possess greater numbers of heterocystous *Cyanobacteria* (i.e. *Scytonema*, *Spirirestis*, and *Nostoc* (Yeager et al., 2006, 2012)) than developing BSC but both young and old BSC are dominated by non-heterocystous *Cyanobacteria* (*Microcoleus vaginatus* or *M. steenstrupii*) (Yeager et al., 2004; Garcia-Pichel et al., 2013). Heterocystous *Cyanobacteria* are the numerically dominant BSC diazotrophs in *nifH* clone libraries (Yeager et al., 2006, 2004, 2012). Eighty-nine percent of 693 *nifH* sequences derived from Colorado Plateau and New Mexico BSC samples as heterocystous cyanobacterial (non-cyanobacterial *nifH* sequences were largely attributed to alpha- and beta- *proteobacteria*) Yeager et al. (2006). However, an early survey of Colorado Plateau BSC *nifH* diversity recovered *nifH* genes related to *Gammaproteobacteria* as well as a clade that included *nifH* genes from the anaerobes *Clostridium pssteurianum*, *Desulfovibrio gigas* and *Chromatium buderii*,

The influence of microbial community membership and structure on BSC N<sub>2</sub>-fixation is an ongoing research question (Belnap, 2013). While the presence/abundance of heterocystous *Cyanobacteria* has been proposed as the mechanism behind increased N<sub>2</sub>-fixation in mature BSC, it is unclear if mature BSC actually fix more N than early successional BSC (see Johnson et al. (2005)). More studies are necessary to elucidate the microbial membership influence on BSC N<sub>2</sub>-fixation and to determine if heterocystous *Cyanobacteria* are the only keystone diazotrophs. The first step in defining structure function relationships with respect to N<sub>2</sub>-fixation is a full accounting of BSC diazotrophs. Towards this end we conducted <sup>15</sup>N<sub>2</sub> DNA stable isotope probing (DNA-SIP) experiments with light, developing Colorado Plateau BSC. DNA-SIP with <sup>15</sup>N<sub>2</sub> has not been attempted with BSC. DNA-SIP provides an accounting of *active* diazotrophs whereas *nifH* clone libraries account for microbes with the genomic potential for N<sub>2</sub>-fixation. Further, we investigate the distribution of these active diazotrophs through collections of SSU rRNA gene sequences from BSC NGS microbial diversity surveys over a range of spatial scales and soil types (Garcia-Pichel et al., 2013; Steven et al., 2013).

### 3 RESULTS

#### 3.1 ORDINATION OF CSCL GRADIENT FRACTION SSU rRNA SEQUENCE COLLECTIONS SHOWS HEAVY FRACTIONS FROM CONTROL AND LABELED CSCL GRADIENTS ARE DIFFERENT

BSC were incubated for 4 days in the presence or absence of  $^{15}\text{N}_2$  and DNA was extracted for DNA-SIP at 2 and 4 days. Fractionation of CsCl gradients permitted separation of DNA on the basis of buoyant density. Ordination of Bray-Curtis (Bray and Curtis, 1957) distances between SSU-rRNA amplicon sequence collections from gradient fractions reveals that labeled gradient fraction (i.e. gradient fractions of DNA from  $^{15}\text{N}_2$  incubations) sequence collections diverge from control (i.e. DNA from incubations without  $^{15}\text{N}_2$ ) at the “heavy” of the CsCl gradients (Figure 1 and Figure S2). Differences among label/control groups with heavy fractions are statistically significant by the Adonis test (p-value: 0.001,  $r^2$ : 0.18) (Anderson, 2001).

#### 3.2 OTUS RESPONSIVE TO $^{15}\text{N}_2$ ARE PRIMARILY *PROTEOBACTERIA* AND *CLOSTRIDIACEAE*

A statistically significant increase in OTU abundance in heavy fractions of  $^{15}\text{N}_2$  labeled samples relative to corresponding control fractions provides evidence for OTUs that have incorporated  $^{15}\text{N}$  into their DNA. Specifically, we compared OTU proportion means between labeled and control samples from heavy gradient fractions using statistics developed to find differentially expressed genes with RNASeq data (McMurdie and Holmes, 2014; Love et al., 2014). OTUs that incorporated  $^{15}\text{N}$  into DNA and increased in buoyant density were identified by rejecting the null hypothesis that the labeled versus control proportion mean ratio for an OTU was below a chosen threshold (see methods). p-values were adjusted by the BH method (Benjamini and Hochberg, 1995) and we used a false discovery rate (FDR) cutoff of 0.10 (typical FDR threshold in gene expression data analysis). A total of 2,127 and 2,160 OTUs were detected in days 2 and 4, respectively, and interrogated for evidence of  $^{15}\text{N}_2$ -labelling. Of these OTUs, only 208 and 233, respectively, passed a sparsity threshold we applied as an independent filtering step to pre-screen out OTUs not likely to produce significant p-values (see Love et al. (2014) for discussion of independent filtering). Of OTUs passing sparsity criteria 38 were found to be enriched significantly in “heavy” fractions relative to control. These OTUs likely incorporated  $^{15}\text{N}$  into DNA ( $^{15}\text{N}_2$  “responders”). Of these 38, 26 are annotated as *Firmicutes*, 9 as *Proteobacteria*, 2 as *Acidobacteria* and 1 as *Actinobacteria* (Figure 3, Figure 2). If the responder OTUs are ranked by descending, moderated proportion mean labeled:control ratios, the top 10 ratios (i.e. the 10 OTUs that were most enriched in the labeled gradients considering only heavy fractions) are either *Firmicutes* (6 OTUs) or *Proteobacteria* (4 OTUs) (Figure 4). Centroid sequences of strongly responding *Proteobacteria* OTUs all share high sequence identity (>98.48%, Table 1) with cultivars from genera known to possess diazotrophs including *Klebsiella*, *Shigella*, *Acinetobacter*, and *Ideonella*. None of the *Firmicutes* OTUs in the top 10 responders share greater than 97% sequence identity with sequences in the LTP database (release 115) (see Table 1). OTUs that passed the sparsity threshold but were not classified as  $^{15}\text{N}$ -responsive were subsequently tested against the null hypothesis that the OTU proportion mean ratio was above the selected threshold. Rejecting the second null would indicate an OTU did *not* incorporate  $^{15}\text{N}$  into biomass. There were 58 and 70 “non-responders” at days 2 and 4, respectively. OTUs that did not pass sparsity or could not be classified as either a responder or non-responder are simply ambiguous with respect to  $^{15}\text{N}$  labelling.

#### 3.3 $^{15}\text{N}$ -RESPONSIVE OTUS IN ENVIRONMENTAL SAMPLES

Five of the 6 *Firmicutes* with the strongest response to  $^{15}\text{N}$ -labelling (Table X) belong in the *Clostridiaceae*. We only observed one of these strongly responding *Clostridiaceae* in the data presented by Garcia-Pichel et al. (2013), “OTU.108” (closest BLAST hit in LTP Release 115 – *Caloramator proteoclasticus*, BLAST

115 %ID 96.94, Accession X90488). OTU.108 was found in two samples both characterized as "light" crust.  
 116 One other *Clostridiaceae* OTU with a proportion mean ratio (labeled:control) p-value less than 0.10 but  
 117 outside the top 10 responders was found in the Garcia-Pichel et al. (2013) data (a "light" crust sample)  
 118 (Figure 2). None of the strongly responding *Clostridiaceae* were found in the sequences provided by Steven  
 119 et al. (2013). *Clostridiaceae* <sup>15</sup>N-responder OTU are not closely related to cultivars. (Table 1, Figure 5).  
 120 One of the proteobacterial OTUs with the strongest <sup>15</sup>N response (Table X) was found in Garcia-Pichel  
 121 et al. (2013) (closest BLAST hit in LTP Release 115, BLAST %ID 100, Accession ZD3440, *Acinetobacter*  
 122 *johnsonii*). None of the strongly responding *Proteobacteria* OTUs were found in the Steven et al. (2013)  
 123 sequences. Responder OTUs were found in Steven et al. (2013) samples 133 times. 83 were in "below  
 124 crust" samples, 50 in crust samples (see Figure 2). Two <sup>15</sup>N-responsive OTUs were found in an extensive  
 125 number of environmental samples (61 of 65 samples from the combined data sets of Garcia-Pichel et al.  
 126 (2013) and Steven et al. (2013)). Both OTUs were annotated as *Acidobacteria* but shared little sequence  
 127 identity to any cultivar SSU rRNA gene sequences in the LTP (Release 115), with best LTP BLAST hits  
 128 of 81.91 and 81.32% identity. Additionally, the <sup>15</sup>N-response for each OTU was weak relative to other  
 129 putative responders (3. Of the remaining 36 stable isotope responder OTUs, only 14 were observed in the  
 130 environmental data (Figure 2, Figure S5).

### 3.4 COMPARING SEQUENCE COLLECTIONS AT "STUDY"-LEVEL

131 We compared the sequences determined in this study to two previous surveys of SSU rRNA amplicons  
 132 from BSC communities: the Garcia-Pichel et al. (2013) and Steven et al. (2013) study. There were 3,079  
 133 OTUs (209,354 total sequences after quality control) in the DNA-SIP data, 3,203 OTUs (129,033 total  
 134 sequences after quality control) in the Garcia-Pichel et al. (2013) study, and 2,481 OTUs (129,358 total  
 135 sequences after quality control) in the Steven et al. (2013) study. Of the 4,340 OTU centroids established  
 136 for this study (including sequences from Steven et al. (2013) and Garcia-Pichel et al. (2013)) 445 have  
 137 matches in the Living Tree Project (LTP) (a collection of 16S gene sequences for all sequenced type  
 138 strains (Yarza et al., 2008)) at greater or equal than 97% sequence identity (LTP version 115). That is, 445  
 139 of 4,340 OTUs (10%) are closely related to cultivars. The DNA-SIP data set shares 56% OTUs with the  
 140 Steven et al. (2013) data and 46% of OTUs with the Garcia-Pichel et al. (2013) data (where total OTUs  
 141 are from the combined data for each pairwise comparison). The Steven et al. (2013) and Garcia-Pichel  
 142 et al. (2013) studies share 46% of OTUs. *Cyanobacteria* and *Proteobacteria* were the top two phylum-  
 143 level sequence annotations for all three studies of BSC. Only the DNA-SIP data had more *Proteobacteria*  
 144 annotations than *Cyanobacteria*. *Proteobacteria* represented the 29.8% of sequence annotations in DNA-  
 145 SIP data as opposed to 17.8% and 19.2% for the Garcia-Pichel et al. (2013) and Steven et al. (2013)  
 146 data, respectively. There is a stark contrast in the total percentage of sequences annotated as *Firmicutes*  
 147 between the raw environmental samples and the DNA-SIP data. *Firmicutes* represent only 0.21% and  
 148 0.23% of total phylum level sequence annotations in the Steven et al. (2013) and Garcia-Pichel et al.  
 149 (2013) studies, respectively (Figure S1). In the DNA-SIP sequence collection *Firmicutes* make up 19% of  
 150 phylum level sequence annotations. Also in sharp contrast for the DNA-SIP versus environmental data is  
 151 the number of putative heterocystous *Cyanobacteria* sequences. Only 0.29% of *Cyanobacteria* sequences  
 152 in the DNA-SIP data are annotated as belonging to "Subsection IV" which is the heterocystous order of  
 153 *Cyanobacteria* in the Silva taxonomic nomenclature (Pruesse et al., 2007). In the Steven et al. (2013) and  
 154 Garcia-Pichel et al. (2013) studies 15% and 23%, respectively, of *Cyanobacteria* sequences are annotated  
 155 as belonging to "Subsection IV".

## 4 DISCUSSION

### 4.1 STUDY-LEVEL DIFFERENCES

156 SIP places focus upon organisms based on isotope incorporation and has the ability to detect activity by  
 157 low abundance members of the community. DNA from OTUs that incorporate <sup>15</sup>N into their biomass



158 moves towards the heavy end of the CsCl gradient and therefore OTUs in “labeled” DNA are enriched  
 159 in the full data pool relative to bulk DNA. Phylum-level taxonomic annotations of  $^{15}\text{N}$ -responsive OTUs  
 160 (i.e. *Firmicutes* and *Proteobacteria*) are enriched in the DNA-SIP data relative to environmental data  
 161 (Figure S1).

## 4.2 ORDINATION OF CSCL GRADIENT FRACTION 16S RRNA GENE SEQUENCE COLLECTIONS

162 The ordination of Bray-Curtis distances between CsCl gradient fraction 16S sequence collections show  
 163 that control fractions differ from labeled fractions in the “heavy” range of the CsCl gradients (Figure S2).  
 164 If each control fraction is paired to the labeled fraction from the same incubation day for which it is closest  
 165 in density, there is a positive and statistically significant correlation between Bray-Curtis distances within  
 166 fraction pairs and density of the pair (see inset Figure S2). Therefore, the “heavy” end of the control and  
 167 labeled gradients differ and the OTUs enriched in the labeled fractions (relative to control) would have  
 168 incorporated  $^{15}\text{N}$  into their DNA during the incubation timeframe.

## 4.3 BSC DIAZOTROPHS IDENTIFIED IN THE STUDY

169 BSC N-fixation has long been attributed to heterocystous *Cyanobacteria* and molecular microbial ecology  
 170 surveys of BSC *nifH* gene content have been consistent with this hypothesis finding cyanobacterial *nifH*  
 171 types to be numerically dominant in *nifH* gene libraries (Yeager et al., 2006, 2004, 2012). Even poorly  
 172 developed BSC samples have yielded predominantly cyanobacterial *nifH* genes (Yeager et al., 2004).  
 173 And, “sub-biocrust” samples have yielded *entirely* heterocystous cyanobacterial *nifH* genes (Yeager et al.,  
 174 2012). It is possible, however, that PCR-driven molecular surveys of *nifH* gene content have been biased  
 175 against non-heterocystous *Cyanobacteria*. In general the *nifH* PCR primers used by Yeager et al. (2006,  
 176 2004, 2012) (“19F” and “nifH3”) for the first round of nested PCR have broad specificity and display at  
 177 least 86% *in silico* coverage for *Proteobacteria*, *Cyanobacteria* and “Cluster III” *nifH* reference sequences  
 178 (Gaby and Buckley, 2012). In the second round of the nested PCR protocol (Yeager et al., 2006, 2004,  
 179 2012), primer “nifH11” is slightly biased against “Cluster III” (50% coverage) but biased in favor of  
 180 *Proteobacteria* (79% *in silico* coverage against 67% for *Cyanobacteria*) and primer “nifH22” matches  
 181 *Proteobacteria*, *Cyanobacteria* and “Cluster III” reference sequences poorly (16%, 23% and 21% *in silico*  
 182 coverage, respectively) (Gaby and Buckley, 2012). Unfortunately, it is difficult to assess or quantify this  
 183 bias (in either direction) without knowing the *nifH* gene content *de novo*. Another potential bias in favor of  
 184 *Cyanobacteria* in BSC *nifH* gene libraries is heterocysts (the specialized N-fixing cells along the trichome  
 185 of filamentous heterocystous *Cyanobacteria* such as *Nostoc* and *Scytonema*) may be overrepresented  
 186 with respect to non-cyanobacterial diazotrophs because heterocysts make up a fraction of cells along a  
 187 trichome and even the non-heterocyst cells in a trichome will possess the *nifH* gene. Polyploidy could  
 188 further exacerbate this bias, as many *Cyanobacteria* are estimated to have multiple genome copies per  
 189 cell (Griese et al., 2011). It should also be noted that *nifH* gene content is not directly extrapolable to  
 190 the taxonomic relative abundances of nitrogenase proteins. Regardless, our results suggest that BSC N-  
 191 fixation may include a significant non-cyanobacterial component that requires further assessment across  
 192 a more comprehensive sampling of BSC types.

193 We did not observe evidence for N-fixation by heterocystous *Cyanobacteria* in the “light” crust samples  
 194 used in this study. One possible explanation for our results is that the “light”, still developing BSC samples  
 195 used in this study possessed too few heterocystous *Cyanobacteria* to statistically evaluate their  $^{15}\text{N}$ -  
 196 incorporation. Indeed, only 0.29% of sequences from this study’s DNA-SIP 16S rRNA gene sequence  
 197 libraries were from heterocystous *Cyanobacteria* (see results) as opposed to 15% and 23% of total  
 198 sequences in the Steven et al. (2013) and Garcia-Pichel et al. (2013) data, respectively. Nonetheless,  
 199 we would still expect even low abundance diazotrophs to show evidence for  $^{15}\text{N}$ -incorporation, provided  
 200 sequence counts were not too sparse in heavy fractions. The OTUs defined by selected heterocystous  
 201 *Cyanobacteria* sequences presented in Yeager et al. (2006), however, all fall below the sparsity threshold

used in our analysis (see methods). Given the sparsity of heterocystous *Cyanobacteria* sequences in the DNA-SIP data set, it is not possible to assess whether heterocystous *Cyanobacteria* incorporated  $^{15}\text{N}$  during the incubation. It should be noted that "light" and in particular "sub-biocrust" samples possess much less heterocystous *Cyanobacteria* in general (Figure S3) so the samples used in this study are not necessarily unrepresentative of typical poorly developed BSC simply because they are lacking heterocystous *Cyanobacteria*.

The OTUs that did appear to incorporate  $^{15}\text{N}$  during the incubation were predominantly *Proteobacteria* and *Firmicutes*. The *Proteobacteria* OTUs for which  $^{15}\text{N}$ -incorporation signal was strongest all shared high sequence identity ( $\geq 98.48\%$  sequence identity) with 16S sequences from cultivars in genera with known diazotrophs (Table 1). The *Firmicutes* that displayed signal for  $^{15}\text{N}$ -incorporation (predominantly *Clostridiaceae*) were not closely related to any cultivars (Table 1, Figure 5). These BSC *Clostridiaceae* diazotrophs represent a gap in culture collections. As culture-based ecophysiological studies have proven useful towards explaining ecological phenomena in BSC 16S rRNA gene sequence libraries (Garcia-Pichel et al., 2013), it would seem that these putative *Clostridiaceae* diazotrophs would be prime candidates for targeted culturing efforts. Assessing the physiological response of these diazotrophic *Clostridiaceae* to temperature would be useful for predicting how climate change will affect the BSC nitrogen budget. *Gamma-proteobacteria* and spore-forming *Firmicutes* are classic opportunistic lineages that would presumably be suited to the boom/bust BSC environment. The compatible solutes produced and secreted by cyanobacteria in response to desiccation and subsequent wetting would create C-rich environment after wetting. Diazotrophs would be uniquely suited to respond quickly in high C:N conditions.

Although too undersampled in the environmental data sets to reach statistical conclusions,  $^{15}\text{N}$ -responsive OTUs were found more often in sub-crust or "light" BSC samples (Figure 2 and Figure S5). This result generates some hypotheses that are counter to prior discussions regarding BSC diazotroph temporal dynamics. Specifically, the transition of BSC from a light colored, developing crust to a dark, mature crust may not mark the *emergence* of diazotrophs in BSC but rather the *transition* of the diazotroph community from heterotroph dominance to cyanobacteria. Additionally, the soil beneath BSC may contribute significantly to the N budget in arid ecosystems.

#### 4.4 SEQUENCING DEPTH

Rarefaction curves of all samples from Steven et al. (2013) and Garcia-Pichel et al. (2013) are still sharply increasing especially for "below crust" samples (Figure S4). Parametric richness estimates of BSC diversity indicate the Steven et al. (2013) and Garcia-Pichel et al. (2013) sequencing efforts recovered on average 40.5% (sd. 9.99%) and 45.5% (sd. 11.6%) of existing 16S OTUs from samples (inset Figure S4), respectively. Further, the Steven et al. (2013) and Garcia-Pichel et al. (2013) sequence collections only share 57.6% of total OTUs found in at least one of the studies. In fact, this study shares more OTUs with Steven et al. (2013), 62.4% of OTUs in the combined data, than the Steven et al. (2013) study shares with Garcia-Pichel et al. (2013). Therefore, is not alarming that few of the  $^{15}\text{N}$ -responsive OTUS were found by Garcia-Pichel et al. (2013) and Steven et al. (2013). Even next-generation sequencing efforts of BSC 16S rRNA genes have only shallowly sampled the full diversity of BSC microbes.

#### 4.5 CONCLUSION

Heterocystous *Cyanobacteria* are key contributors to the BSC N-budget, but, the  $^{15}\text{N}$ -responsive OTUs found in this study and the *nifH* gene sequences from Steppe et al. (1996) in addition to the N-fixation rate data presented by Johnson et al. (2005) suggest there may be significant non-cyanobacterial BSC diazotrophs specifically within the *Clostridiaceae* and *Proteobacteria*. It seems clear that heterocystous *Cyanobacteria* increase in abundance with BSC age (Yeager et al., 2004). It is less clear if this transition marks the emergence of diazotrophy versus a re-structuring of the BSC diazotroph community from

one dominated by *Firmicutes* and *Proteobacteria* to one predominantly heterocystous *Cyanobacteria*. DNA-SIP is a valuable tool in the molecular microbial ecologist's toolbox for identifying members of microbial community functional guilds (Neufeld et al., 2007). PCR-based surveys of diagnostic marker genes and DNA-SIP are both used to connect microbial phylogenetic types to microbial activities, but they occupy a non-overlapping set of strengths and weaknesses. DNA-SIP does not focus on a specific diagnostic marker but does identify *active* players in the studied process (i.e. N-fixation). Combined these tools can powerfully reveal connections between ecosystem membership/structure and function. Here we supplement previous surveys of BSC *nifH* diversity, a diagnostic marker PCR-driven approach, with  $^{15}\text{N}_2$  DNA-SIP. While we do not confirm previous results, we expand knowledge of BSC diazotroph diversity. Predicting BSC N-fixation with respect to climate change, altered precipitation regimes and physical disturbance requires a careful accounting of diazotrophs including non-cyanobacterial types.

## 5 MATERIALS AND METHODS

### 5.1 BSC SAMPLING AND INCUBATION CONDITIONS

Light crust samples ( $37.5\text{ cm}^2$ , average mass 35 g) were incubated in sealed chambers under controlled atmosphere and in the light for 4 days. Crusts were dry prior to time zero and were wetted at initiation of experiment. Treatments included control air (unenriched headspace) and enriched air ( $>98\%$  atom  $^{15}\text{N}_2$ ) headspace. Samples were taken at 2 days and 4 days incubation. Acetylene reduction rates were measured daily. DNA was extracted from 1 g of crust. Samples were taken from Green Butte, Arizona as previously described (site CP3, Beraldi-Campesi et al. (2009)). All samples were from light crusts as described by Johnson et al. (2005).

### 5.2 DNA EXTRACTION

DNA from each sample was extracted using a MoBio PowerSoil DNA Isolation Kit (following manufacturers protocol, but substituting a 2 minute bead beating for the vortexing step), and then gel purified. Extracts were quantified using PicoGreen nucleic acid quantification dyes (Molecular Probes).

### 5.3 DNA-SIP

Gradient density centrifugation of DNA was undertaken in 4.7 mL polyallomer centrifuge tubes in a TLA-110 fixed angle rotor (both Beckman Coulter) in CsCl gradients with an average density of 1.725 g/mL. Average density for all prepared gradients was checked with an AR200 refractometer before runs. Between 2.5-5  $\mu\text{g}$  of DNA extract was added to the CsCl solution (15mM Tris-HCl, pH 8; 15mM EDTA; 15mM KCl), and gradients were run under conditions of 20C for 67 hours at 55,000 rpm (Buckley et al.). Centrifuged gradients were fractionated from bottom to top in 36 equal fractions of 100  $\mu\text{L}$ , using a syringe pump as described Manfield et al. (2002). The density of each fraction was determined using an AR200 refractometer modified to accommodate 5ul samples (Buckley et al.). DNA in each fraction was desalted on a filter plate (PALL, AcroPrep Advance 96 Filter Plate, Product Number 8035), using four washes with 300 $\mu\text{L}$  TE per fraction. After each wash, the filter plate was spun at 500 g for 10 minutes, with a final spin of 20 minutes. Fractions were resuspended in 50  $\mu\text{L}$  of TE buffer.

### 5.4 PCR, LIBRARY NORMALIZATION AND DNA SEQUENCING

Barcoded PCR of bacterial and archaeal 16S rRNA genes, in preparation for 454 Pyrosequencing, was carried out using primer set 515F/806R (Walters et al., 2011) (primers purchased from Integrated DNA Technologies). The primer 806R contained an 8 bp barcode sequence, a "TC" linker, and a Roche 454 B sequencing adaptor, while the primer 515F contained the Roche 454 A sequencing adapter. Each 25  $\mu\text{L}$  reaction contained 1x PCR Gold Buffer (Roche), 2.5 mM  $\text{MgCl}_2$ , 200  $\mu\text{M}$  of each of the four

dNTPs (Promega), 0.5 mg/mL BSA (New England Biolabs), 0.3  $\mu$ M of each primers, 1.25 U of Amplitaq Gold (Roche), and 8  $\mu$ L of template. Each sample was amplified in triplicate. Thermal cycling occurred with an initial denaturation step of 5 minutes at 95C, followed by 40 cycles of amplification (20s at 95C, 20s at 53C, 30s at 72C), and a final extension step of 5 min at 72C. Triplicate amplicons were pooled and purified using Agencourt AMPure PCR purification beads, following manufacturers protocol. Once cleaned, amplicons were quantified using PicoGreen nucleic acid quantification dyes (Molecular Probes) and pooled together in equimolar amounts. Samples were sent to the Environmental Genomics Core Facility at the University of South Carolina (now Selah Genomics) to be run on a Roche FLX 454 pyrosequencing machine.

## 5.5 DATA ANALYSIS

All code to take raw sequencing data through the presented figures can be found at:

[http://nbviewer.ipython.org/github/chuckpr/NSIP\\_data\\_analysis](http://nbviewer.ipython.org/github/chuckpr/NSIP_data_analysis)

**5.5.1 Sequence quality control** Sequences were initially screened by maximum expected errors at a specific read length threshold (Edgar, 2013) which has been shown to be as effective as denoising reads with respect to removing pyrosequencing errors. Specifically, reads were first truncated to 230 nucleotides (nt) (all reads shorter than 230 nt were discarded) and any read that exceeded a maximum expected error threshold of 1.0 was removed. After truncation and max expected error trimming, 91% of original reads remained. The first 30 nt representing the forward primer and barcode on high quality, truncated reads were trimmed. Remaining reads were taxonomically annotated using the "UClust" taxonomic annotation framework in the QIIME software package (Caporaso et al., 2010; Edgar, 2010) with cluster seeds from Silva SSU rRNA database (Pruesse et al., 2007) 97% sequence identity OTUs as reference (release 111Ref). Reads annotated as "Chloroplast", "Eukaryota", "Archaea", "Unassigned" or "mitochondria" were culled from the dataset. Finally, reads were aligned to the Silva reference alignment provided by the Mothur software package (Schloss et al., 2009) using the Mothur NAST aligner (DeSantis et al., 2006). All reads that did not appear to align to the expected amplicon region of the SSU rRNA gene were discarded. Quality control parameters removed 34,716 of 258,763 raw reads.

**5.5.2 Sequence clustering** Sequences were distributed into OTUs using the UParse methodology (Edgar, 2013). Specifically, cluster seeds were identified using USearch with a collection of non-redundant reads sorted by count as input. The sequence identity threshold for establishing a new OTU centroid was 97%. After initial cluster centroid selection, select 16S rRNA gene sequences trimmed to the same alignment positions as the other centroids from Yeager et al. (2006) were added to the centroid collection. Specifically, Yeager et al. (2006) Colorado Plateau or Moab, Utah sequences were added which included the 16S rRNA gene sequences for *Calothrix* MCC-3A (accession DQ531700.1), *Nostoc commune* MCT-1 (accession DQ531903), *Nostoc commune* MFG-1 (accession DQ531699.1), *Scytonema hyalinum* DC-A (accession DQ531701.1), *Scytonema hyalinum* FGP-7A (accession DQ531697.1), *Spirirestis rafaelsensis* LQ-10 (accession DQ531696.1). Centroid sequences that matched selected Yeager et al. (2006) sequences with greater than to 97% sequence identity were subsequently removed from the centroid collection. With USearch/UParse, potential chimeras are identified during OTU centroid selection and are not allowed to become cluster centroids effectively removing chimeras from the read pool. All quality controlled reads were then mapped to cluster centroids at an identity threshold of 97% again using USearch. 95.6% of quality controlled reads could be mapped to centroids. Unmapped reads do not count towards sample counts and are essentially removed from downstream analyses. The USearch software version for cluster generation was 7.0.1090.

**5.5.3 Merging data from this study, Garcia-Pichel et al. (2013), and Steven et al. (2013)** As only sequences without corresponding quality scores were publicly available from Garcia-Pichel et al. (2013) and Steven et al. (2013), these data sets were only quality screened by determining if they covered the



328 expected region of the 16S rRNA gene (described above). All data (this study, Garcia-Pichel et al. (2013)  
 329 and Steven et al. (2013)) were included as input to USearch for OTU centroid selection and subsequent  
 330 mapping to OTU centroids.

331 *5.5.4 Phylogenetic tree* The alignment for the "*Clostridiaceae*" phylogeny was created using SSU-  
 332 Align which is based on Infernal (Nawrocki and Eddy, 2013; Nawrocki et al., 2009). Columns in  
 333 the alignment that were not included in the SSU-Align covariance models or were aligned with poor  
 334 confidence (less than 95% of characters in a position had posterior probability alignment scores of  
 335 at least 95%) were masked for phylogenetic reconstruction. Additionally, the alignment was trimmed  
 336 to coordinates such that all sequences in the alignment began and ended at the same positions. The  
 337 "*Clostridiaceae*" tree included all top BLAST hits (parameters below) for  $^{15}\text{N}$  *Clostridiaceae* responders  
 338 in the Living Tree Project database (Yarza et al., 2008) in addition to BLAST hits within a sequence  
 339 identity threshold of 97% to  $^{15}\text{N}$  responders from the Silva SSURef\_NR SSU rRNA database (Pruesse  
 340 et al., 2007). Only one SSURef\_NR115 hit per study per OTU ("study" was determined by "title" field)  
 341 was selected for the tree. FastTree (Price et al., 2010) was used to build the tree and support values are  
 342 SH-like scores reported by FastTree.

343 *Placement of short sequences into backbone phylogeny* Short sequences were mapped to the reference  
 344 backbone using pplacer (Matsen et al., 2010) (default parameters). pplacer finds the edge placements that  
 345 maximize phylogenetic likelihood. Prior to being mapped to the reference tree, short sequences were  
 346 aligned to the reference alignment using Infernal (Nawrocki et al., 2009) against the same SSU-Align  
 347 covariance model used to align reference sequences.

348 *5.5.5 BLAST searches* BLAST searches were done with the "blastn" program from BLAST+ toolkit  
 349 (Camacho et al., 2009) version 2.2.29+. Default parameters were always employed and the BioPython  
 350 (Cock et al., 2009) BLAST+ wrapper was used to invoke the blastn program. Pandas (McKinney, 2012)  
 351 and dplyr (Wickham and Francois, 2014) were used to parse and munge BLAST output tables.

352 *5.5.6 Identifying OTUs that incorporated  $^{15}\text{N}$  into their DNA* SIP is a culture-independent approach  
 353 towards defining identity-function connections in microbial communities (Buckley, 2011; Neufeld et al.,  
 354 2007). Microbes incubated in the presence of  $^{13}\text{C}$  or  $^{15}\text{N}$  labeled substrates can incorporate the stable  
 355 heavy isotope into biomass if they participate in the substrate's transformation. Stable isotope labeled  
 356 nucleic acids can then be separated from unlabeled by buoyant density in a CsCl gradient. As the buoyant  
 357 density of a macromolecule is dependent on many factors in addition to stable isotope incorporation  
 358 (e.g. GC-content in nucleic acids (Youngblut and Buckley, 2014)), labeled nucleic acids from one  
 359 microbial population may have the same buoyant density of unlabeled nucleic acids from another (i.e.  
 360 each population's nucleic acids would be found at the same point along a density gradient although  
 361 only one population's nucleic acids are labeled). Therefore it is imperative to compare density gradients  
 362 with nucleic acids from heavy stable isotope incubations to gradients from "control" incubations where  
 363 everything mimics the experimental conditions except that unlabeled substrates are used (and all DNA  
 364 would be unlabeled). By contrasting "heavy" density gradient fractions in experimental density gradients  
 365 (hereafter referred to as "labeled" gradients) against heavy fractions in control gradients, the identities of  
 366 microbes with labeled nucleic acids can be determined

367 We used an RNA-Seq differential expression statistical framework (Love et al., 2014) to find OTUs  
 368 enriched in heavy fractions of labeled gradients relative to corresponding density fractions in control  
 369 gradients (for review of RNA-Seq differential expression statistics applied to microbiome OTU count data  
 370 see McMurdie and Holmes (2014)). We use the term differential abundance (coined by McMurdie and  
 371 Holmes (2014)) to denote OTUs that have different proportion means across sample classes (in this case  
 372 the only sample class is labeled/control). CsCl gradient fractions were categorized as "heavy" or "light".  
 373 The heavy category denotes fractions with density values above 1.725 g/mL. Since we are only interested

in enriched OTUs (labeled versus control), we used a one-sided z-test for differential abundance (the null hypothesis is the labeled:control proportion mean ratio for an OTU is less than a selected threshold). P-values were corrected with the Benjamini and Hochberg method (Benjamini and Hochberg, 1995). We selected a  $\log_2$  fold change null threshold of 0.25 (or a labeled:control proportion mean ratio of 1.19). DESeq2 was used to calculate the moderated  $\log_2$  fold change of labeled:control proportion mean ratios and corresponding standard errors. Mean ratio moderation allows for reliable ratio ranking such that high variance and likely statistically insignificant mean ratios are appropriately shrunk and subsequently ranked lower than they would be as raw ratios. To summarize, OTUs with high moderated labeled:control proportion mean ratios have higher proportion means in heavy fractions of labeled gradients relative to heavy fractions of control gradients, and therefore have likely incorporated  $^{15}\text{N}$  into their DNA during the incubation.

Although DNA-SIP is a powerful technique, analysis of DNA-SIP data is not without ambiguities. One limitation is the discrete, selected boundary in the form of a adjusted p-value threshold (or false discovery rate) that marks which OTUs we consider to be enriched in the heavy fractions of labeled CsCl gradients (and thus have likely incorporated  $^{15}\text{N}$  into their DNA during the incubation). In reality the metric we use to quantify the magnitude of an OTU's response to a stable isotope is continuous, and there is only an artificial boundary between which OTUs appear to have "responded" and which OTUs have unknown response. For this reason, we have presented all the OTUs that satisfy our "response" criteria but focused on the most strongly responding OTUs. As with any hypothesis-based statistical test, care should be taken when interpreting the significance of results where p-values are near the selected threshold for rejecting the null hypothesis.

**5.5.7 Ordination** Principal coordinate ordinations depict the relationship between samples at each time point (day 2 and 4). Bray-Curtis distances were used as the sample distance metric for ordination. The Phyloseq (McMurdie and Holmes, 2014) wrapper for Vegan (Oksanen et al., 2013) (both R packages) was used to compute sample values along principal coordinate axes. GGplot2 (Wickham, 2009) was used to display sample points along the first and second principal axes. Adonis tests Anderson (2001) were done with default number of permutations (1000).

## 5.6 RICHNESS ANALYSES

Rarefaction curves were created using bioinformatics modules in the PyCogent Python package (Knight et al., 2007). Parametric richness estimates were made with CatchAll using only the best model for total OTU estimates (Bunge, 2010).

## REFERENCES

- Marti J. Anderson. A new method for non-parametric multivariate analysis of variance. *Austral Ecology*, 26(1):32–46, Feb 2001. doi: 10.1111/j.1442-9993.2001.01070.pp.x. URL <http://dx.doi.org/10.1111/j.1442-9993.2001.01070.pp.x>.
- J. Belnap. Factors Influencing Nitrogen Fixation and Nitrogen Release in Biological Soil Crusts. In *Biological Soil Crusts: Structure Function, and Management*, pages 241–261. Springer Science + Business Media, 2001. doi: 10.1007/978-3-642-56475-8\_19. URL [http://dx.doi.org/10.1007/978-3-642-56475-8\\_19](http://dx.doi.org/10.1007/978-3-642-56475-8_19).
- J. Belnap. Factors Influencing Nitrogen Fixation and Nitrogen Release in Biological Soil Crusts. In Jayne Belnap and Otto L. Lange, editors, *Biological Soil Crusts: Structure, Function, and Management*, volume 150 of *Ecological Studies*, pages 241–261. Springer Berlin Heidelberg, 2003. ISBN 978-3-540-43757-4. doi: 10.1007/978-3-642-56475-8\_19. URL [http://dx.doi.org/10.1007/978-3-642-56475-8\\_19](http://dx.doi.org/10.1007/978-3-642-56475-8_19).

- J. Belnap, R. Prasse, and K.T. Harper. Influence of Biological Soil Crusts on Soil Environments and Vascular Plants. In Jayne Belnap and Otto L. Lange, editors, *Biological Soil Crusts: Structure, Function, and Management*, volume 150 of *Ecological Studies*, pages 281–300. Springer Berlin Heidelberg, 2003. ISBN 978-3-540-43757-4. doi: 10.1007/978-3-642-56475-8\_21. URL [http://dx.doi.org/10.1007/978-3-642-56475-8\\_21](http://dx.doi.org/10.1007/978-3-642-56475-8_21).
- Jayne Belnap. Nitrogen fixation in biological soil crusts from southeast Utah USA. *Biology and Fertility of Soils*, 35(2):128–135, Apr 2002. doi: 10.1007/s00374-002-0452-x. URL <http://dx.doi.org/10.1007/s00374-002-0452-x>.
- Jayne Belnap. Some Like It Hot, Some Not. *Science*, 340(6140):1533–1534, 2013. doi: 10.1126/science.1240318. URL <http://www.sciencemag.org/content/340/6140/1533.short>.
- Yoav Benjamini and Yosef Hochberg. Controlling the False Discovery Rate: A Practical and Powerful Approach to Multiple Testing. *Journal of the Royal Statistical Society. Series B (Methodological)*, 57(1):289–300, 1995. ISSN 00359246. doi: 10.2307/2346101. URL <http://dx.doi.org/10.2307/2346101>.
- H. Beraldi-Campesi, H. E. Hartnett, A. Anbar, G. W. Gordon, and F. Garcia-Pichel. Effect of biological soil crusts on soil elemental concentrations: implications for biogeochemistry and as traceable biosignatures of ancient life on land. *Geobiology*, 7(3):348–359, jun 2009. doi: 10.1111/j.1472-4669.2009.00204.x. URL <http://dx.doi.org/10.1111/j.1472-4669.2009.00204.x>.
- J. Roger Bray and J. T. Curtis. An Ordination of the Upland Forest Communities of Southern Wisconsin. *Ecological Monographs*, 27(4):325, Oct 1957. doi: 10.2307/1942268. URL <http://dx.doi.org/10.2307/1942268>.
- Daniel H. Buckley. Stable Isotope Probing Techniques Using  $^{15}\text{N}$ . In *Stable Isotope Probing and Related Technologies*, pages 129–147. American Society of Microbiology, jan 2011. doi: 10.1128/9781555816896.ch7. URL <http://dx.doi.org/10.1128/9781555816896.ch7>.
- DH Buckley, V Huangyutitham, SF Hsu, and TA Nelson. Stable isotope probing with  $^{15}\text{N}_2$  reveals novel noncultivated diazotrophs in soil. *Appl Environ Microbiol*, 73:3196–204.
- John Bunge. Estimating the Number of Species with Catchall. In *Biocomputing 2011*, pages 121–130. WORLD SCIENTIFIC, nov 2010. doi: 10.1142/9789814335058\_0014. URL [http://dx.doi.org/10.1142/9789814335058\\_0014](http://dx.doi.org/10.1142/9789814335058_0014).
- C Camacho, G Coulouris, V Avagyan, N Ma, J Papadopoulos, K Bealer, and TL Madden. BLAST+: architecture and applications. 10:421, Dec 2009.
- JG Caporaso, J Kuczynski, J Stombaugh, K Bittinger, FD Bushman, EK Costello, N Fierer, AG Pea, JK Goodrich, JI Gordon, GA Huttley, ST Kelley, D Knights, JE Koenig, RE Ley, CA Lozupone, D McDonald, BD Muegge, M Pirrung, J Reeder, JR Sevinsky, PJ Turnbaugh, WA Walters, J Widmann, T Yatsunenko, J Zaneveld, and R Knight. QIIME allows analysis of high-throughput community sequencing data. 7:335–6, 2010.
- PJ Cock, T Antao, JT Chang, BA Chapman, CJ Cox, A Dalke, I Friedberg, T Hamelryck, F Kauff, B Wilczynski, and Hoon MJ de. Biopython: freely available Python tools for computational molecular biology and bioinformatics. 25:1422–3, 2009.
- TZ Jr DeSantis, P Hugenholtz, K Keller, EL Brodie, N Larsen, YM Piceno, R Phan, and GL Andersen. NAST: a multiple sequence alignment server for comparative analysis of 16S rRNA genes. 34:W394–9, 2006.
- RC Edgar. Search and clustering orders of magnitude faster than BLAST. 26:2460–1, 2010.
- RC Edgar. UPARSE: highly accurate OTU sequences from microbial amplicon reads. 10:996–8, 2013.
- R. D. Evans and J. Belnap. Long-Term Consequences of Disturbance on Nitrogen Dynamics in an Arid Ecosystem. *Ecology*, 80(1):150–160, Jan 1999. doi: 10.1890/0012-9658(1999)080[0150:lrcodo]2.0.co;2. URL [http://dx.doi.org/10.1890/0012-9658\(1999\)080\[0150:LTCODO\]2.0.CO;2](http://dx.doi.org/10.1890/0012-9658(1999)080[0150:LTCODO]2.0.CO;2).
- R. D. Evans and O. L. Lange. Biological Soil Crusts and Ecosystem Nitrogen and Carbon Dynamics. In *Biological Soil Crusts: Structure Function, and Management*, pages 263–279. Springer Science + Business Media, 2001. doi: 10.1007/978-3-642-56475-8\_20. URL [http://dx.doi.org/10.1007/978-3-642-56475-8\\_20](http://dx.doi.org/10.1007/978-3-642-56475-8_20).

- John Christian Gaby and Daniel H. Buckley. A Comprehensive Evaluation of {PCR} Primers to Amplify the {nifH} Gene of Nitrogenase. {PLOS} {ONE}, 7(7):e42149, jul 2012. doi: 10.1371/journal.pone.0042149. URL <http://dx.doi.org/10.1371/journal.pone.0042149>.
- F. Garcia-Pichel, S. L. Johnson, D. Youngkin, and J. Belnap. Small-Scale Vertical Distribution of Bacterial Biomass and Diversity in Biological Soil Crusts from Arid Lands in the Colorado Plateau. *Microbial Ecology*, 46(3):312–321, Nov 2003a. doi: 10.1007/s00248-003-1004-0. URL <http://dx.doi.org/10.1007/s00248-003-1004-0>.
- F. Garcia-Pichel, V. Loza, Y. Marusenko, P. Mateo, and R. M. Potrafka. Temperature Drives the Continental-Scale Distribution of Key Microbes in Topsoil Communities. *Science*, 340(6140):1574–1577, Jun 2013. doi: 10.1126/science.1236404. URL <http://dx.doi.org/10.1126/science.1236404>.
- Ferran Garcia-Pichel, Jayne Belnap, Susanne Neuer, and Ferdinand Schanz. Estimates of global cyanobacterial biomass and its distribution. *Algological Studies*, 109(1):213–227, 2003b.
- Marco Griese, Christian Lange, and Jrg Soppa. Ploidy in cyanobacteria. *FEMS Microbiology Letters*, 323(2):124–131, sep 2011. doi: 10.1111/j.1574-6968.2011.02368.x. URL <http://dx.doi.org/10.1111/j.1574-6968.2011.02368.x>.
- SL Johnson, CR Budinoff, J Belnap, and F Garcia-Pichel. Relevance of ammonium oxidation within biological soil crust communities. 7:1–12, 2005.
- A. Karnieli, R.F. Kokaly, N.E. West, and R.N. Clark. Remote Sensing of Biological Soil Crusts. In Jayne Belnap and OttoL. Lange, editors, *Biological Soil Crusts: Structure, Function, and Management*, volume 150 of *Ecological Studies*, pages 431–455. Springer Berlin Heidelberg, 2003. ISBN 978-3-540-43757-4. doi: 10.1007/978-3-642-56475-8\_31. URL [http://dx.doi.org/10.1007/978-3-642-56475-8\\_31](http://dx.doi.org/10.1007/978-3-642-56475-8_31).
- Rob Knight, Peter Maxwell, Amanda Birmingham, Jason Carnes, J Gregory Caporaso, Brett C Easton, Michael Eaton, Micah Hamady, Helen Lindsay, Zongzhi Liu, Catherine Lozupone, Daniel McDonald, Michael Robeson, Raymond Sammut, Sandra Smit, Matthew J Wakefield, Jeremy Widmann, Shandy Wikman, Stephanie Wilson, Hua Ying, and Gavin A Huttley. {PyCogent}: a toolkit for making sense from sequence. *Genome Biol*, 8(8):R171, 2007. doi: 10.1186/gb-2007-8-8-r171. URL <http://dx.doi.org/10.1186/gb-2007-8-8-r171>.
- M. I. Love, W. Huber, and S. Anders. Moderated estimation of fold change and dispersion for {RNA}-Seq data with {DESeq}2. Technical report, feb 2014. URL <http://dx.doi.org/10.1101/002832>.
- Frederick A Matsen, Robin B Kodner, and E Virginia Armbrust. pplacer: linear time maximum-likelihood and Bayesian phylogenetic placement of sequences onto a fixed reference tree. *BMC Bioinformatics*, 11(1):538, 2010. doi: 10.1186/1471-2105-11-538. URL <http://dx.doi.org/10.1186/1471-2105-11-538>.
- Wes McKinney. pandas: Python Data Analysis Library. Online, 2012. URL <http://pandas.pydata.org/>.
- PJ McMurdie and S Holmes. Waste not, want not: why rarefying microbiome data is inadmissible. 10:e1003531, 2014.
- EP Nawrocki and SR Eddy. Infernal 1.1: 100-fold faster RNA homology searches. 29:2933–5, Nov 2013.
- EP Nawrocki, DL Kolbe, and SR Eddy. Infernal 1.0: inference of RNA alignments. 25:1335–7, May 2009.
- JD Neufeld, J Vohra, MG Dumont, T Lueders, M Manefield, MW Friedrich, and JC Murrell. DNA stable-isotope probing. 2:860–6, 2007.
- Jari Oksanen, F. Guillaume Blanchet, Roeland Kindt, Pierre Legendre, Peter R. Minchin, R. B. O’Hara, Gavin L. Simpson, Peter Solymos, M. Henry H. Stevens, and Helene Wagner. *vegan: Community Ecology Package*, 2013. URL <http://CRAN.R-project.org/package=vegan>. R package version 2.0-10.
- MN Price, PS Dehal, and AP Arkin. FastTree 2—approximately maximum-likelihood trees for large alignments. 5:e9490, Mar 2010.



- 519 E Pruesse, C Quast, K Knittel, BM Fuchs, W Ludwig, J Peplies, and FO Glckner. SILVA: a comprehensive  
 520 online resource for quality checked and aligned ribosomal RNA sequence data compatible with ARB.  
 521 35:7188–96, 2007.
- 522 PD Schloss, SL Westcott, T Ryabin, JR Hall, M Hartmann, EB Hollister, RA Lesniewski, BB Oakley,  
 523 DH Parks, CJ Robinson, JW Sahl, B Stres, GG Thallinger, Horn DJ Van, and CF Weber.  
 524 Introducing mothur: open-source, platform-independent, community-supported software for describing  
 525 and comparing microbial communities. 75:7537–41, 2009.
- 526 T.F. Steppe, J.B. Olson, H.W. Paerl, R.W. Litaker, and J. Belnap. Consortial N<sub>2</sub> fixation: a strategy  
 527 for meeting nitrogen requirements of marine and terrestrial cyanobacterial mats. *FEMS Microbiology*  
 528 *Ecology*, 21(3):149–156, Nov 1996. doi: 10.1111/j.1574-6941.1996.tb00342.x. URL [http://dx.](http://dx.doi.org/10.1111/j.1574-6941.1996.tb00342.x)  
 529 [doi.org/10.1111/j.1574-6941.1996.tb00342.x](http://dx.doi.org/10.1111/j.1574-6941.1996.tb00342.x).
- 530 Blaire Steven, La Verne Gallegos-Graves, Jayne Belnap, and Cheryl R. Kuske. Dryland soil microbial  
 531 communities display spatial biogeographic patterns associated with soil depth and soil parent material.  
 532 *FEMS Microbiol Ecol*, 86(1):101–113, May 2013. doi: 10.1111/1574-6941.12143. URL [http:](http://dx.doi.org/10.1111/1574-6941.12143)  
 533 [//dx.doi.org/10.1111/1574-6941.12143](http://dx.doi.org/10.1111/1574-6941.12143).
- 534 WA Walters, JG Caporaso, CL Lauber, D Berg-Lyons, N Fierer, and R Knight. PrimerProspector: de novo  
 535 design and taxonomic analysis of barcoded polymerase chain reaction primers. 27:1159–61, Apr 2011.
- 536 Hadley Wickham. *ggplot2: elegant graphics for data analysis*. Springer New York, 2009. ISBN 978-0-  
 537 387-98140-6. URL <http://had.co.nz/ggplot2/book>.
- 538 Hadley Wickham and Romain Francois. *dplyr: dplyr: a grammar of data manipulation*, 2014. URL  
 539 <http://CRAN.R-project.org/package=dplyr>. R package version 0.2.
- 540 Pablo Yarza, Michael Richter, Jörg Peplies, Jean Euzeby, Rudolf Amann, Karl-Heinz Schleifer, Wolfgang  
 541 Ludwig, Frank Oliver Glöckner, and Ramon Rosselló-Móra. The All-Species Living Tree project: A  
 542 16S rRNA-based phylogenetic tree of all sequenced type strains. *Systematic and Applied Microbiology*,  
 543 31(4):241–250, Sep 2008. doi: 10.1016/j.syapm.2008.07.001. URL [http://dx.doi.org/10.](http://dx.doi.org/10.1016/j.syapm.2008.07.001)  
 544 [1016/j.syapm.2008.07.001](http://dx.doi.org/10.1016/j.syapm.2008.07.001).
- 545 Chris M. Yeager, Jennifer L. Kornosky, Rachael E. Morgan, Elizabeth C. Cain, Ferran Garcia-Pichel,  
 546 David C. Housman, Jayne Belnap, and Cheryl R. Kuske. Three distinct clades of cultured heterocystous  
 547 cyanobacteria constitute the dominant N<sub>2</sub>-fixing members of biological soil crusts of the Colorado  
 548 Plateau USA. *FEMS Microbiology Ecology*, 60(1):85–97, 2006. doi: 10.1111/j.1574-6941.2006.00265.  
 549 x. URL <http://dx.doi.org/10.1111/j.1574-6941.2006.00265.x>.
- 550 Chris M. Yeager, Cheryl R. Kuske, Travis D. Carney, Shannon L. Johnson, Lawrence O. Ticknor, and  
 551 Jayne Belnap. Response of Biological Soil Crust Diazotrophs to Season Altered Summer Precipitation,  
 552 and Year-Round Increased Temperature in an Arid Grassland of the Colorado Plateau, USA. *Front.*  
 553 *Microbio.*, 3, 2012. doi: 10.3389/fmicb.2012.00358. URL [http://dx.doi.org/10.3389/](http://dx.doi.org/10.3389/fmicb.2012.00358)  
 554 [fmicb.2012.00358](http://dx.doi.org/10.3389/fmicb.2012.00358).
- 555 CM Yeager, JL Kornosky, DC Housman, EE Grote, J Belnap, and CR Kuske. Diazotrophic community  
 556 structure and function in two successional stages of biological soil crusts from the Colorado Plateau  
 557 and Chihuahuan Desert. 70:973–83, 2004.
- 558 ND Youngblut and DH Buckley. Intra-genomic variation in G+C content and its implications for DNA  
 559 stable isotope probing (DNA-SIP). Aug 2014.

## 6 FIGURES AND LONG TABLES

**Table 1.** <sup>15</sup>N responders BLAST against Living Tree Project

OTU ID	Species Names	BLAST %ID
OTU.342	<i>Acinetobacter johnsonii</i>	100.0
OTU.263	<i>Azospirillum picis</i>	98.48
OTU.137	<i>Azospirillum rugosum</i> , <i>A. lipoferum</i>	98.98
OTU.3	<i>Bacillus azotoformans</i>	100.0
OTU.140	<i>Bacillus korensis</i> , <i>B. beringensis</i>	100.0
OTU.108	<i>Caloramator proteoclasticus</i>	96.94
OTU.61	<i>Clostridium drakei</i> , <i>C. carboxidivorans</i>	95.92
OTU.11	<i>Clostridium drakei</i> , <i>C. carboxidivorans</i>	95.94
OTU.1673	<i>Clostridium drakei</i> , <i>C. carboxidivorans</i>	95.9
OTU.1747	<i>Clostridium hydrogeniformans</i> , <i>C. algidicarnis</i>	94.36
OTU.327	<i>Clostridium hydrogeniformans</i> , <i>C. amylolyticum</i>	94.92
OTU.330	<i>Clostridium lundense</i>	96.94
OTU.75	<i>Clostridium lundense</i>	96.97
OTU.2175	<i>Clostridium paraputrificum</i> , <i>C. lundense</i>	95.96
OTU.643	<i>Clostridium tagluense</i> , <i>C. estertheticum</i> subsp. <i>laramiense</i> , <i>C. estertheticum</i> subsp. <i>estertheticum</i> , <i>C. bowmanii</i> , <i>C. algoriphilum</i>	97.45
OTU.17	<i>Clostridium thiosulfatireducens</i> , <i>C. sulfidigenes</i> , <i>C. subterminale</i>	95.45
OTU.176	<i>Delftia tsuruhatensis</i> , <i>D. lacustris</i>	100.0
OTU.78	<i>Desulfocella halophila</i> , <i>Bryobacter aggregatus</i>	80.31
OTU.55	<i>Desulfocella halophila</i> , <i>Bryobacter aggregatus</i>	81.03
OTU.2404	<i>Domibacillus robiginosus</i>	99.49
OTU.3712	<i>Eubacterium tarantellae</i> , <i>Clostridium perfringens</i>	96.43
OTU.4167	<i>Fonticella tunisiensis</i>	93.43
OTU.4037	<i>Fonticella tunisiensis</i>	93.85
OTU.57	<i>Fonticella tunisiensis</i> , <i>Caloramator proteoclasticus</i>	93.88
OTU.575	<i>Gracilibacter thermotolerans</i>	94.42
OTU.37	<i>Ilyobacter delafieldii</i> , <i>Clostridium nitrophenolicum</i> , <i>C. aciditolerans</i>	96.43
OTU.14	<i>Pantoea rwandensis</i> , <i>P. rodasii</i> , <i>Kluyvera intermedia</i> , <i>K. cryocrescens</i> , <i>Klebsiella variicola</i> , <i>K. pneumoniae</i> subsp. <i>rhinoscleromatis</i> , <i>K. pneumoniae</i> subsp. <i>pneumoniae</i> , <i>Erwinia aphidicola</i> , <i>Enterobacter soli</i> , <i>E. ludwigii</i> , <i>E. kobei</i> , <i>E. hormaechei</i> , <i>E. cloacae</i> subsp. <i>dissolvens</i> , <i>E. cancerogenus</i> , <i>E. asburiae</i> , <i>E. amnigenus</i> , <i>E. aerogenes</i> , <i>Buttiauxella warmboldiae</i> , <i>B. noackiae</i> , <i>B. izardii</i> , <i>B. agrestis</i>	99.49
OTU.259	<i>Parasporobacterium paucivorans</i>	98.47
OTU.321	<i>Pseudomonas beteli</i>	100.0
OTU.54	<i>Shigella sonnei</i> , <i>S. flexneri</i> , <i>Escherichia fergusonii</i> , <i>E. coli</i>	100.0
OTU.116	<i>Streptomyces ziwulingensis</i> , <i>S. viridodiatstaticus</i> , <i>S. viridochromogenes</i> , <i>S. violascens</i> , <i>S. violarius</i> , <i>S. violaceus</i> , <i>S. violaceorubidus</i> , <i>S. violaceoruber</i> , <i>S. violaceolatus</i> , <i>S. violaceochromogenes</i> , <i>S. vinaceusdrappus</i> , <i>S. variabilis</i> , <i>S. tuius</i> , <i>S. tricolor</i> , <i>S. thinghirensis</i> , <i>S. tendae</i> , <i>S. spectabilis</i> , <i>S. silaceus</i> , <i>S. rutgersensis</i> , <i>S. rubrogriseus</i> , <i>S. roseoviolaceus</i> , <i>S. rochei</i> , <i>S. resistomycificus</i> , <i>S. plicatus</i> , <i>S. phaeoluteichromatogenes</i> , <i>S. parvulus</i> , <i>S. paradoxus</i> , <i>S. pactum</i> , <i>S. olivaceus</i> , <i>S. mutabilis</i> , <i>S. misionensis</i> , <i>S. minutiscleroticus</i> , <i>S. matensis</i> , <i>S. massasporeus</i> , <i>S. marokkonensis</i> , <i>S. malachitospinus</i> , <i>S. luteogriseus</i> , <i>S. longispororuber</i> , <i>S. lienomycini</i> , <i>S. levis</i> , <i>S. labedae</i> , <i>S. koyangensis</i> , <i>S. jietaisiensis</i> , <i>S. janthinus</i> , <i>S. intermedius</i> , <i>S. iakyrus</i> , <i>S. hydrogenans</i> , <i>S. humiferus</i> , <i>S. hawaiiensis</i> , <i>S. griseorubens</i> , <i>S. griseoincarnatus</i> , <i>S. griseoflavus</i> , <i>S. griseochromogenes</i> , <i>S. griseoaurantiacus</i> , <i>S. gougerotii</i> , <i>S. glomeratus</i> , <i>S. ghanaensis</i> , <i>S. geysiriensis</i> , <i>S. fulvissimus</i> , <i>S. flavofungini</i> , <i>S. flaveolus</i> , <i>S. eurythermus</i> , <i>S. erythrogriseus</i> , <i>S. diastaticus</i> subsp. <i>diastaticus</i> , <i>S. dahestanicus</i> , <i>S. collinus</i> , <i>S. coerulescens</i> , <i>S. coeruleorubidus</i> , <i>S. coelicoflavus</i> , <i>S. coelestis</i>	100.0

**Figure 1.** Ordination of heavy gradient fraction sequence collections by Bray-Curtis distances.

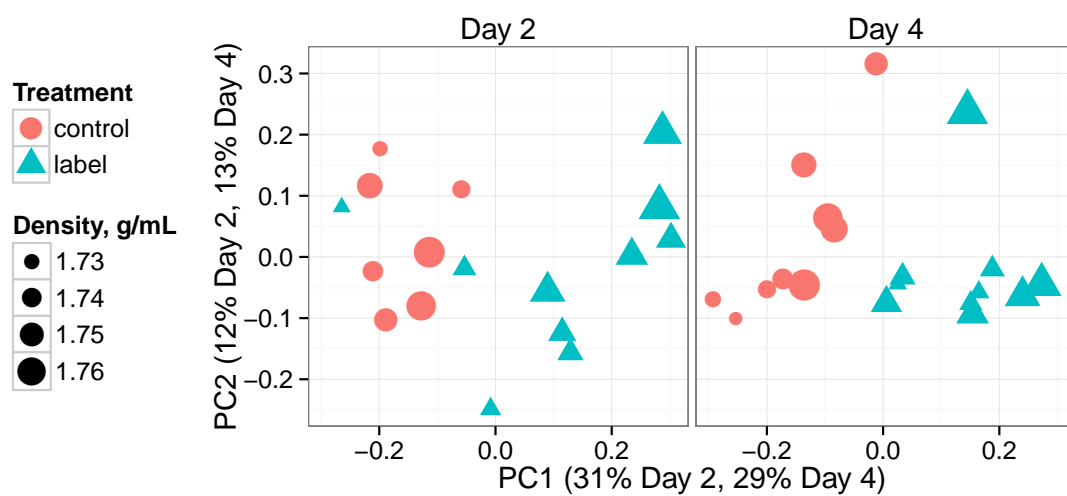


**Figure 2.** Phylogenetic trees of OTUs passing sparsity threshold for selected phyla. *A*) Point denotes OTU is classified as a  $^{15}\text{N}$  “responder”. *B*) Heatmap of moderated  $\log_2$  proportion mean ratios (labeled:control gradients) for each OTU at each incubation day. High values indicate  $^{15}\text{N}$  incorporation. *C*) Presence/absence of OTUs (black indicates presence) in lichen, light, or dark environmental samples (Garcia-Pichel et al., 2013). *D*) Presence/absence of OTUs (black indicates presence) in crust and below crust samples (Steven et al., 2013).

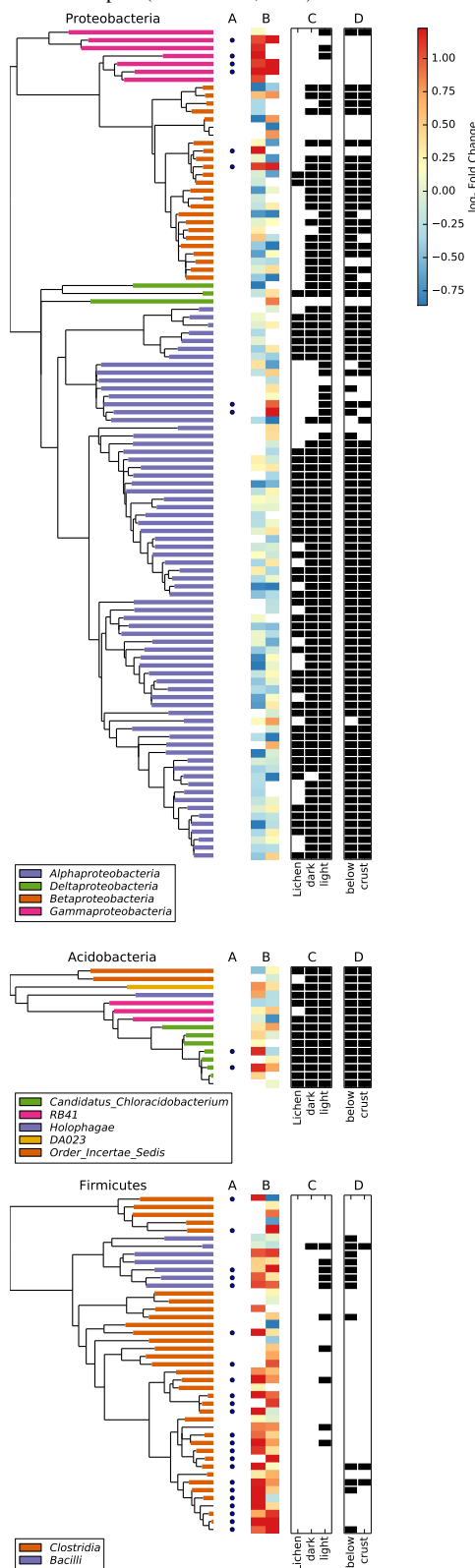




**Figure 3.** Moderated  $\log_2$  of proportion mean ratios for labeled versus control gradients (heavy fractions only, densities  $\geq 1.725$  g/mL). All OTUs found in at least 62.5% of heavy fractions at a specific incubation day are shown. Red color denotes a proportion mean ratio that has a corresponding adjusted p-value below a false discovery rate of 10% (the null model is that the proportion mean is ratio is below 0.25). The horizontal line is the proportion mean threshold for the null model, 0.25. The inset figure summarizes the taxonomy of OTUs that with proportion mean ratio p-values under 0.10 for at least one time point.



**Figure 4.** Relative abundance values in heavy fractions (density greater or equal to 1.725 g/mL) for the top 10  $^{15}\text{N}$  "responders" (putative diazotrophs, see results for selection criteria of top 10) at each incubation day. See Table 1 for BLAST results of top 10 responders against the LTP database (release 115). Point area is proportional to CsCl gradient fraction density, and color signifies control (red) or labeled (blue) treatment.



Phylogenetic tree showing the relationships between various bacterial strains, primarily *Clostridium* species, based on 16S rDNA sequences. The tree is rooted with *Bacillus subtilis* subsp. *subtilis* AJ276351 as the outgroup. Bootstrap values are indicated at the nodes. The scale bar represents 0.01 substitutions per site.

Key strains and their accession numbers shown in the tree include:

- Bacillus subtilis* subsp. *subtilis* AJ276351
- Caloramator proteoclasticus* X90488
- Fonticella tunisiensis* HE604099
- Clostridium algidicarnis* AF127023
- Clostridium amylolyticum* EUP37903
- Clostridium hydrogeniformans* DQ196623
- Clostridium paraputrificum* X75907
- Clostridium perfringens* CP000246
- Eubacterium tarantellae* FR733677
- Clostridium carboxidivorans* FR733710
- Clostridium drakei* Y18813
- Clostridium aciditolerans* DQ114945
- Clostridium nitrophenolicum* AM261414
- Clostridium lundense* AY858804
- Clostridium subterminale* AF241844
- Clostridium sulfidigenes* EF199998
- Clostridium thiosulfatireducens* AY024332
- Clostridium tagluense* DQ296031
- Clostridium bowmanii* AJ506119
- Clostridium algariphilum* AY117755
- Clostridium estertheticum* subsp. *laramiense* AJ506115
- Clostridium estertheticum* subsp. *estertheticum* S46734

## 7 SUPPLEMENTAL FIGURES



**Figure S1.** Distribution of sequences into top 9 phyla (phyla ranked by sum of all sequence annotations).



**Figure S2.** Ordination of Bray-Curtis sample pairwise distances for each incubation time. Point area is proportional to the density of the CsCl gradient fraction for each sequence library, and color/shape reflects control (red triangles) or labeled (blue circles) treatment. Inset shows Bray-Curtis distances for paired control versus labeled CsCl gradient fractions (i.e. fractions from the same incubation day and same density) against the density of the pair (p-value:  $4.526 \times 10^{-5}$ ,  $r^2$ : 0.434).



**Figure S3.** Relative abundance of selected heterocystous cyanobacterial OTUs with centroids from sequences described in Yeager et al. (2006) (see methods for selection criteria) in Steven et al. (2013) data set.



**Figure S4.** Rarefaction curves for all samples presented by Garcia-Pichel et al. (2013) and Steven et al. (2013). Inset is boxplot of estimated sampling effort for all samples in Garcia-Pichel et al. (2013) and Steven et al. (2013) (number of observed OTUs divided by number of CatchAll Bunge (2010) estimated total OTUs)





**Figure S5.** Counts of "responder" OTU occurrences in samples from Steven et al. (2013) and Garcia-Pichel et al. (2013). Steven et al. (2013) collected BSC samples (25 samples total) and samples from soil beneath BSC (17 samples total, "below" column in figure). Garcia-Pichel et al. (2013) collected samples from "dark" (9 samples total) and "light" (12 samples total) crusts in addition to "lichen" (2 samples total) dominated crusts.

